DIRECT STRAIN ESTIMATION IN ULTRASOUND ELASTOGRAPHY USING A NOVEL DYNAMIC PROGRAMMING APPROACH

Hossein Khodadadi, Amir G. Aghdam and Hassan Rivaz

Department of Electrical and Computer Engineering, Concordia University, Montreal, Canada.

ABSTRACT

Quasi-static elastography methods often calculate the displacement field from ultrasound data and calculate strain by performing spatial derivative of the displacement field. In this paper, a strain imaging technique called SHORTCUT is introduced in which the strain field is estimated directly from the RF data using a novel dynamic programming (DP) technique. The DP cost function is formulated in terms of *strain* and incorporates similarity of echo amplitudes and *strain continuity* into a cost function. This is in contrast to previous work wherein the cost function was formulated in terms of *displacement* and enforced *displacement continuity*. This approach has several advantages. First, a much smaller search range for the displacement derivative will cover a much larger search range of the displacement field. This will substantially reduce the computational complexity of DP. Second, the new framework substantially reduces the bias introduced by the displacement continuity constraint. And third, the strain is directly estimated from DP and no spatial derivation step is needed. Our results on phantom and *in vivo* patient data show that SHORTCUT substantially outperforms previous work.

Index Terms— Ultrasound, Elastography, Dynamic Programming, Strain Estimation.

1. INTRODUCTION

Ultrasound elastography aims to reveal the mechanical properties of tissue and has numerous applications in both diagnosis and surgical planning [1–3]. The displacement estimation techniques in quasi-static elastography can be predominantly categorized into window-based [1, 4–7] and optimization-based [1, 7–13] techniques. Window-based methods are sensitive to signal decorrelation and need to compromise between better spatial resolution with small windows and higher accuracy with larger windows. The optimization-based methods exploit the prior information of motion continuity in tissues and therefore are robust to signal decorrelation. They substantially reduce both jitter error and practically eliminate peak hopping. In [9] a dynamic programming analytical minimization (DPAM) technique is proposed which estimates 2D displacement field. The cost function of DPAM has been improved in GLUE [14] to the sum of the echo amplitude similarities and motion discontinuity penalizations in the frame of RF data. In both DPAM and GLUE, the integer displacements from DP [8] are needed as the initial solution of the regularized cost function.

The aforementioned technique all calculate the displacement field first and estimate strain in the next step by performing the spatial gradient of the displacement field, a process which amplifies the noise and can blur the strain image. We proposed an edge-preserving method that somehow alleviated this problem [15]. The other disadvantage is that they do not exploit the information of the RF data in the strain estimation step, and only rely on displacement data. However, Recent work has tried to address this problem by directly estimating strain from ultrasound data [5, 16–22]. Most of these techniques calculate the strain image by applying local or global adaptive temporal stretching of the signals in the time or frequency domain. In [5] and [16], a two-step method is proposed to use optical flow with local warping to calculate displacements and strain, simultaneously. To compensate for the signal decorrelation due to the non-axial motion of tissue scatterers, a direct average strain estimation (DASE) method using the weighted nearest neighbor method is proposed in [17]. Despite improving the results, current direct strain estimation techniques suffer from at least one of the following shortcomings: (1) Producing strain images with an acceptable SNR and CNR requires global 2D search, which is computationally expensive. Therefore, existing global search methods are not suitable for real-time applications. (2) Regularized algorithms entail enforcing displacement continuity, and as such, favor constant displacement estimates. This leads to substantial underestimation of the displacement derivative, i.e. strain.

To overcome these challenges, we introduce a 2-D strain imaging technique by minimizing a cost function that incorporates the similarity of echo amplitudes and strain continuity. The cost function directly optimizes for the strain. The proposed technique, which is referred to as **SHORT-**

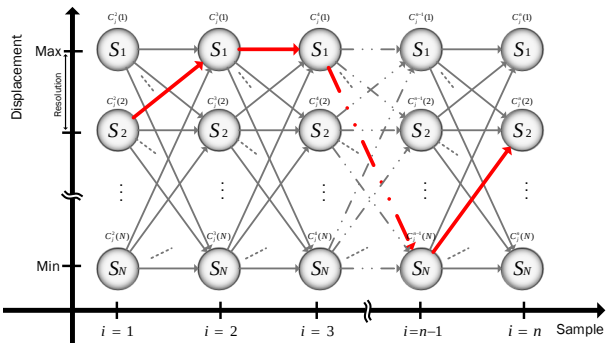

Fig. 1. A depiction of the Viterbi algorithm.

CUT (me**SH**ing **O**f g**R**adien**T** in DP for dire**C**t **U**ltrasound elas**T**ography), directly produces the strain images from RF data using a novel dynamic programming (DP) approach. Unlike the standard DP algorithms which discretize the decision space (displacement field) and search in the space of piecewise constant functions, the proposed DP method discretizes the gradient of the decision space (strain field) and searches the space of continuous piecewise-linear functions.

The advantages of SHORTCUT compared to previous work are four-fold. First, it eliminates the displacement differentiation block and performs direct strain estimation. Second, it performs global optimization for the strain. Third, regularization is enforced on displacement derivative, and as such, bias in the strain estimates are substantially reduced. And fourth, the gradient of decision space is considerably smaller than the decision space, leading to a large reduction of the computational complexity of DP.

This paper is organized as follows. In the next section, we provide details of the proposed SHORTCUT algorithm. The effectiveness of the proposed method is then investigated in Section 3 through phantom experiments and *in vivo* patient data and compared with a previous work. Conclusions and avenues for future work are provided in Section 4.

2. METHODS

2.1. BACKGROUND

DP is a global optimization method based on Bellman's principle of optimality [23] for solving a complex problem. It breaks the problem down into a collection of simpler subproblems wherein each subproblem corresponds to a discrete decision, solving each of those subproblems just once, storing their solutions (memoization) and reusing them next time the same subproblem occurs. The decisions should follow each other sequentially and the cost corresponding to each decision should only depend on the previous and not the future decisions (causality). This approach saves computation time at the expense of a modest expenditure in storage space.

Assume two consecutive ultrasound Radio-Frequency (RF) echo field $I_1(i,j) : i \in \mathbb{N}^{\leq m} \times j \in \mathbb{N}^{\leq n} \to \mathbb{R}$ and $I_2(i,j) : i \in \mathbb{N}^{\leq m} \times j \in \mathbb{N}^{\leq n} \to \mathbb{R}$ are collected before and after the tissue undergoes some deformation. Define $A^{m\times n} \in \mathbb{R}$ and $L^{m\times n} \in \mathbb{R}$ as the axial and lateral displacement matrices (the out-of-plane motion is not considered here) where each of their elements $a_{i,j}$ and $l_{i,j}$ satisfy $\|a_{i,j}\| \leq a_{\max}$ and $\|l_{i,j}\| \leq l_{\max}$, and $a_{\max}$ and $l_{\max}$ are the maximum possible axial and lateral displacement estimates, respectively. Assume the set $\mathscr{A} = \{a_k : \|a_k\| < a^{\max}\}_{k=1}^{N}$ partitions the axial displacement's range into $N+1$ intervals. Similarly, assume the set $\mathscr{L} = \{l_k : \|l_k\| < l^{\max}\}_{k=1}^{M}$ partitions the lateral displacement's range into $M+1$ intervals. In [8], DP is used to find the displacement matrices A and L in integer precision. Assuming that ultrasound images consist of n A-lines, we define data and smoothness terms as follows:

$$D(i,j,a_{i,j},l_{i,j}) = \left|I_1(i,j) - I_2((i+a_{i,j}, j+l_{i,j})\right|, \quad (1)$$

$$R(a_{i,j},l_{i,j},a_{i-1,j},l_{i-1,j}) = (a_{i,j}-a_{i-1,j})^2 + (l_{i,j}-l_{i-1,j})^2. \quad (2)$$

The cost function at the ith sample of the jth A-line is

$$C_i^j(a_{i,j},l_{i,j}) = D(i,j,a_{i,j},l_{i,j}) + \min_{\delta_a,\delta_l} \left\{ \frac{C_{i-1,j}(\delta_a,\delta_l) + C_{i,j-1}(\delta_a,\delta_l)}{2} + \alpha R(a_{i,j},l_{i,j},\delta_a,\delta_l) \right\}. \quad (3)$$

As shown in Figure 1, costs will be calculated at each state $S_k \in \mathscr{A} \times \mathscr{L}$ going forward in two adjacent data points. The cost in each state (circles) is determined by Eq. (3), which is the minimum cost of reaching that state from any previous step state. To save computing time, these values will be stored in a 3D array $C_i^j(k)$ and the Viterbi algorithm can efficiently trace back the global optimum solution from $i = n$ to $i = 1$ (See the thick line path in Figure 1). Inspired by this approach in the following subsection we introduce a fast, robust and accurate direct 2-D strain imaging technique using a novel DP configuration. Unlike the standard DP algorithm which discretizes the decision space (displacement field) and searches in the space of piecewise constant displacement functions, The proposed DP discretizes the gradient of the decision space (strain field) and searches the space of continuous piecewise linear displacement functions. In other words, *the main idea of SHORTCUT is to change the vertical axis in Figure 1 from displacement to strain.* This is outlined in the next section.

2.2. SHORTCUT

Assume the possible axial strain values $s_{i,j}$ satisfy $\|s_{i,j}\| \leq s_{\max}$. Let also the set $\mathscr{S} = \{s_k : \|s_k\| < s^{\max}\}_{k=1}^{N}$ partition the axial strain's range into $N+1$ intervals. The displacement field is needed to calculate the similarity measure (Eq. 1) in the cost function and the main idea of the new DP method is to discretize the gradient domain (strain) instead of displacement. Therefore, the proposed method needs to integrate the

strain field to generate the displacement field. Hence, the displacement of the first (top) sample of RF data is needed to perform the integral. Fortunately, the first sample in axial line always has zero displacement since the probe is connected to the tissue (i.e. there is no relative vertical motion between the probe and tissue surface). However, no such information is available in the lateral direction since the probe can slip on the tissue. Therefore, the possible states in Eq. 1 are combination of discretized axial strain and lateral displacement i.e. $\mathscr{S} \times \mathscr{L}$. Lateral displacement always has much lower SNR and CNR than axial since the displacement in the lateral direction is very small and also because the resolution of the ultrasound is low in the lateral direction. Therefore it is only computed to improve the axial displacement which means that subsample estimation in the lateral direction is not necessary. Therefore, the new DP framework does not search for lateral strain and searches for lateral displacement similar to previous work [9, 14]. Similar to Eq. 3, the new DP cost function consists of data and regularization terms. They are both formulated as the sum of absolute differences (SAD), which is computationally efficient and is robust to outliers [24]. We set the data and regularization terms as follows:

$$D_{ij}(s_{i,j}, l_{i,j}) = \frac{|I_1(ij) - I_2(i + D(s_{ij}), j + l_{ij})|}{I_1^{\text{env}}(ij)}, \qquad (4)$$

$$R_{ij}(s_{ij}, l_{ij}, \delta_s, \delta_l) = \alpha_a |s_{ij} - \delta_s| + \alpha_l |l_{ij} - \delta_l|, \qquad (5)$$

where $D(s_{ij}) = a_{ij} = \sum_{k=0}^{i} s_{kj}$ is the axial displacement and $s_{0j} = 0$ and I_1^{env} is the envelope of I_1 used for normalization of the error. We then define the DP cost function as follows:

$$C_i^j(s_{ij}, l_{ij}) = D_{ij} + \min_{\delta_s, \delta_l} \left[C_j^{i-1}(\delta_s, \delta_l) + R_{ij} \right]. \qquad (6)$$

Note that minimization of the above cost function will provide the axial strain and lateral displacement fields on the j^{th} axial line. These values are guaranteed to provide the global minimum of the cost function [23].

3. EXPERIMENTAL RESULTS

For experimental evaluation, RF data is acquired from an Antares Siemens system (Issaquah, WA) at the center frequency of $6.67MHz$ with a VF10-5 linear array at a sampling rate of $40MHz$ at Johns Hopkins Hospital, which is available online [9]. This data was collected with approved ethics. In this section, phantom results and patient trials of both SHORTCUT and GLUE methods are presented and compared. The strain fields are calculated using the proposed method and are compared with the GLUE method [14]. The unitless metric signal-to-noise ratio (SNR) and contrast to noise ratio (CNR) are also calculated to better assess the performance of the methods according to [25]

$$CNR = \frac{C}{N} = \sqrt{\frac{2(\bar{s}_b - \bar{s}_t)^2}{\sigma_b^2 + \sigma_t^2}}, \quad SNR = \frac{\bar{s}}{\sigma}, \qquad (7)$$

Table 1. Comparison of the result of two methods. The SNR is calculated for the background window.

Exp.	Method	SNR	CNR
	GLUE	42.23	8.66
Phantom	SHORTCUT	95.89	68.57
	Improvement %	**127**%	**692**%
	GLUE	8.97	3.27
Patient 1	SHORTCUT	12.44	10.2
	Improvement %	**39**%	**212**%
	GLUE	6.29	4.44
Patient 2	SHORTCUT	27.22	28.42
	Improvement %	**333**%	**540**%

where σ_t^2 and σ_b^2 are the spatial strain variance of the target and background, $\bar{s}_t$ and $\bar{s}_b$ are the spatial strain average of the target and background, and $\bar{s}$ and σ are the spatial average and variance of a window in the strain image, respectively. The results are smoothed in the lateral direction using a simple 1D Gaussian filter.

SHORTCUT is currently implemented as MATLAB MEX functions in C++. Given different initial settings, it takes a few milliseconds to a few seconds to run on a standard PC with a 4^{th} generation Intel Core i7 at 3.4 GHz. Our implementation can be optimized to yield substantial improvements in the running time.

3.1. Phantom Results

An elastography phantom (CIRS elastography phantom, Norfolk, VA) is compressed 0.2 inches axially using a linear stage, resulting in an average strain of 2%. The Young's elasticity modulus of the background and the lesion under compression are respectively $33kPa$ and $56kPa$. The axial strain is calculated using both SHORTCUT and GLUE methods. Visual comparison of the results of Fig 2 (a) and (b) shows that SHORTCUT produces an image with sharper edges as well as lower noise levels. To provide quantitative values, SNR is calculated in the four background windows B1 to B4 (Fig 2 (a)-(b)), and the average results are reported in Table 1. Similarly, CNR is calculated between T1 and B1 to B4, and the average results are shown in Table 1. The results of this table show that SNR and CNR are improved by respectively 127% and 692% with SHORTCUT.

3.2. *In-vivo* Results

The *in-vivo* data is acquired from two patients undergoing open surgical radio-frequency thermal ablation for primary or secondary liver cancers. This data is collected at Johns Hopkins Hospital. Figures 2(c)-(f) compare the axial strain images of the SHORTCUT with that of GLUE for the two patients. In both of the axial strain images of different patients, SHORTCUT outperforms GLUE in terms of CNR and SNR

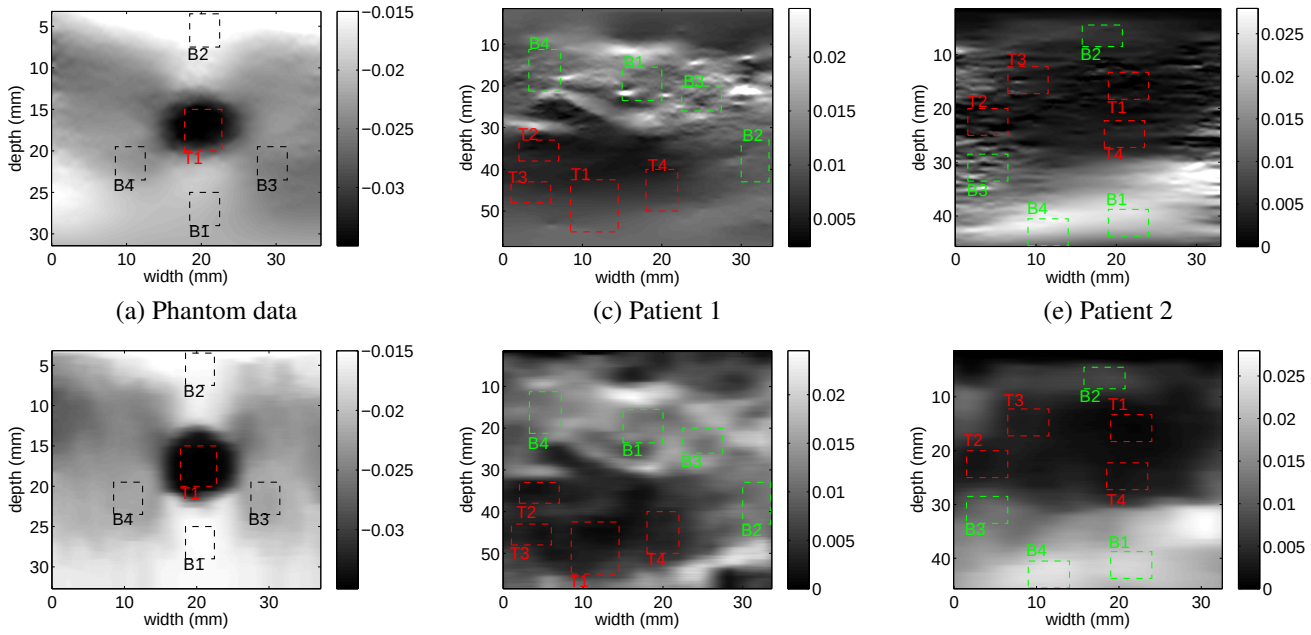

(a) Phantom data (c) Patient 1 (e) Patient 2

(b) Phantom data (d) Patient 1 (f) Patient 2

Fig. 2. The estimated axial strain in phantom and *in-vivo* data. First and second rows correspond to GLUE and SHORTCUT, respectively. Target windows are marked in T and Background windows are marked in B.

especially in the upper and lower quarter of the image which is over-smoothed in GLUE. This over-smoothing is due to the regularization term in GLUE, which biases the estimates to constant displacement. SNR is calculated in the four background windows B1 to B4. CNR is calculated between all combinations of target windows T1 to T4 and background windows B1 to B4, resulting in 16 estimates. The average SNR and CNR results are shown in Table 1, which shows very large improvements in both SNR and CNR. Although GLUE has failed on some local regions, the proposed SHORTCUT method finds the global optimal solution and therefore substantially outperforms GLUE.

4. CONCLUSIONS

In this paper a 2-D strain imaging technique called SHORTCUT is introduced which directly produces the strain images from RF data using a novel dynamic programming (DP) technique. Unlike the standard DP algorithm which discretizes the decision space (displacement field) and searches in the space of piecewise constant functions, the proposed DP discretizes the gradient of the decision space (strain field) and searches in the space of continuous piecewise linear functions. The phantom and patient results show a substantial improvement in both SNR and CNR of the estimated strain image which is mainly the consequence of three major paradigm shifts compared to the available strain estimation techniques in the literature: (1) Eliminating the displacement differentiation block. (2) Performing global optimization rather than local optimization. (3) Regularizing strain values to reduce strain underestimation bias. Furthermore, searching in the strain space reduces the search range, and allows us to perform DP for the entire image in real-time. Finally, DP is a discrete optimization technique that guarantees to find global minimum, and as such, is substantially more robust than continuous optimization techniques used in GLUE and DPAM.

ACKNOWLEDGMENT

This work has been supported by the Natural Sciences and Engineering Research Council of Canada (NSERC) under Grants RGPIN-2017-262127 and RGPIN-2015-04136.

The liver data was collected at Johns Hopkins Hospital, and the PI's were E. Boctor and M. Choti. The authors would like to thank them for allowing us to use the data. We also thank anonymous reviewers for their constructive feedback.

5. REFERENCES

[1] T. J Hall, P. E Barboneg, A. A Oberai, J. Jiang, J.-F. Dord, S. Goenezen, and T. G Fisher, "Recent results in nonlinear strain and modulus imaging," *Current medical imaging reviews*, vol. 7, no. 4, pp. 313–327, 2011.

[2] J.-L. Gennisson, T. Deffieux, M. Fink, and M. Tanter, "Ultrasound elastography: principles and techniques," *Diagnostic and interventional imaging*, vol. 94, no. 5, pp. 487–495, 2013.

[3] K. Parker, M. Doyley, and D. Rubens, "Corrigendum:

Imaging the elastic properties of tissue: the 20 year perspective," *Physics in Medicine and Biology*, vol. 57, no. 16, p. 5359, 2012.

[4] J. Ophir, S. Alam, B. Garra, F. Kallel, E. Konofagou, T. Krouskop, and T. Varghese, "Elastography," *Annu. Rev. Biomed. Eng.*, vol. 213, pp. 203–233, Nov. 1999.

[5] X. Pan, K. Liu, J. Shao, J. Gao, L. Huang, J. Bai, and J. Luo, "Performance comparison of rigid and affine models for motion estimation using ultrasound radio-frequency signals," *IEEE trans. UFFC*, vol. 62, no. 11, pp. 1928–1943, 2015.

[6] R. Zahiri-Azar and S. E. Salcudean, "Motion estimation in ultrasound images using time domain cross correlation with prior estimates," *IEEE Trans. Biomed. Eng.*, vol. 53, no. 10, pp. 1990–2000, 2006.

[7] L. Yuan and P. C. Pedersen, "Analytical phase-tracking-based strain estimation for ultrasound elasticity," *IEEE transactions on ultrasonics, ferroelectrics, and frequency control*, vol. 62, no. 1, pp. 185–207, 2015.

[8] H. Rivaz, E. Boctor, P. Foroughi, R. Zellars, G. Fichtinger, and G. Hager, "Ultrasound elastography: a dynamic programming approach," *Medical Imaging, IEEE Transactions on*, vol. 27, no. 10, pp. 1373–1377, 2008.

[9] H. Rivaz, E. M. Boctor, M. A. Choti, and G. D. Hager, "Real-time regularized ultrasound elastography," *Medical Imaging, IEEE Transactions on*, vol. 30, no. 4, pp. 928–945, Apr 2011.

[10] C. Pellot-Barakat, F. Frouin, M. Insana, and A. Herment, "Ultrasound elastography based on multiscale estimations of regularized displacement fields," *IEEE Trans Med Imaging*, vol. 23, pp. 153–163, . 2004.

[11] H. Rivaz, E. M. Boctor, M. A. Choti, and G. D. Hager, "Ultrasound elastography using multiple images," *Medical image analysis*, vol. 18, no. 2, pp. 314–329, 2014.

[12] J. Jiang and T. J. Hall, "A generalized speckle tracking algorithm for ultrasonic strain imaging using dynamic programming," *Ultrasound in medicine & biology*, vol. 35, no. 11, pp. 1863–1879, 2009.

[13] S. S. Furuie and F. M. Cardoso, "Estimation of deformations in ultrasound images using dynamic programming." in *Image Processing: Algorithms and Systems/Parallel Processing for Imaging Applications*, 2012, p. 82951K.

[14] H. S. Hashemi and H. Rivaz, "Global time-delay estimation in ultrasound elastography," *IEEE Transactions on Ultrasonics, Ferroelectrics, and Frequency Control*, vol. 64, no. 10, pp. 1625–1636, Oct 2017.

[15] H. Khodadadi, A. G. Aghdam, and H. Rivaz, "Edge-preserving ultrasonic strain imaging with uniform precision," in *2015 37th Annual International Conference of the IEEE Engineering in Medicine and Biology Society (EMBC)*, Aug 2015, pp. 3835–3838.

[16] X. Pan, J. Gao, S. Tao, K. Liu, J. Bai, and J. Luo, "A two-step optical flow method for strain estimation in elastography: Simulation and phantom study," *Ultrasonics*, vol. 54, no. 4, pp. 990–996, 2014.

[17] M. A. Hussain, E. M. A. Anas, S. K. Alam, S. Y. Lee, and M. K. Hasan, "Direct and gradient-based average strain estimation by using weighted nearest neighbor cross-correlation peaks," *IEEE transactions on ultrasonics, ferroelectrics, and frequency control*, vol. 59, no. 8, pp. 1713–1728, 2012.

[18] M. Omidyeganeh, Y. Xiao, M. O. Ahmad, and H. Rivaz, "Estimation of strain elastography from ultrasound radio-frequency data by utilizing analytic gradient of the similarity metric," *IEEE Transactions on Medical Imaging*, vol. 36, no. 6, pp. 1347–1358, June 2017.

[19] T. Varghese, E. Konofagou, J. Ophir, S. Alam, and M. Bilgen, "Direct strain estimation in elastography using spectral cross-correlation," *Ultrasound in medicine & biology*, vol. 26, no. 9, pp. 1525–1537, 2000.

[20] S. R. Ara, F. Mohsin, F. Alam, S. A. Rupa, S. Y. Lee, M. K. Hasan, and R. Awwal, "Phase-based direct average strain estimation for elastography," *IEEE transactions on ultrasonics, ferroelectrics, and frequency control*, vol. 60, no. 11, pp. 2266–2283, 2013.

[21] S. K. Alam, F. L. Lizzi, T. Varghese, E. J. Feleppa, and S. Ramachandran, "Adaptive spectral strain estimators for elastography," *Ultrasonic imaging*, vol. 26, no. 3, pp. 131–149, 2004.

[22] U. Bae and Y. Kim, "Direct phase-based strain estimator for ultrasound tissue elasticity imaging," in *Engineering in Medicine and Biology Society, 2004. IEMBS'04. 26th Annual International Conference of the IEEE*, vol. 1. IEEE, 2004, pp. 1345–1348.

[23] R. Bellman, "The theory of dynamic programming," *Bull. Amer. Math. Soc.*, vol. 60, no. 6, pp. 503–515, 11 1954. [Online]. Available: http://projecteuclid.org/euclid.bams/1183519147

[24] P. J. Huber, "Robust statistics. 1981."

[25] J. Ophir, S. K. Alam, B. Garra, F. Kallel, E. Konofagou, T. Krouskop, and T. Varghese, "Elastography: ultrasonic estimation and imaging of the elastic properties of tissues," *Journal of Engineering in Medicine*, vol. 213, no. 3, pp. 203–233, 1999.